

High bandwidth (50 MHz) low offset (200 μ V) rail-to-rail 5 V op-amp


 TSV791
SOT23-5

 TSV792
DFN8 2x2 mm

 TSV792
MiniSO8

 TSV792
SO8

Features

- Gain bandwidth product 50 MHz, unity gain stable
- Slew rate 30 V/ μ s
- Low input offset voltage 50 μ V typ., 200 μ V max.
- Low input bias current: 2 pA typ.
- Low input voltage noise density 6.5 nV/ $\sqrt{\text{Hz}}$ @ 10 kHz
- Wide supply voltage range: 2.2 V to 5.5 V
- Rail-to-rail input and output
- Extended temperature range: - 40 $^{\circ}$ C to +125 $^{\circ}$ C
- Automotive grade version available
- Benefits:
 - Accuracy of measurement virtually unaffected by noise or input bias current
 - Signal conditioning for high frequencies

Applications

- High bandwidth low-side and high-side current sensing
- Photodiode transimpedance amplification
- A/D converters input buffers
- Power management in solar-powered systems
- Power management in automotive applications

Maturity status link

TSV791, TSV792

Related products

| | |
|------------------|---|
| TSZ181 TSZ182 | Zero drift amplifiers with more power savings (3 MHz) |
| TSB712 | 36 V high-bandwidth amplifiers (6 MHz) |
| TSB7192 | 36 V high-bandwidth amplifiers (20 MHz) |

Description

The TSV791 and TSV792 are single and dual 50 MHz-bandwidth unity-gain-stable amplifiers. The rail-to-rail input stage and the slew rate of 30 V/ μ s make the TSV791 and TSV792 ideal for low-side current measurement. The excellent accuracy provided by maximum input voltage of 200 μ V allows amplifying accurately small-amplitude input signal. The TSV79x can operate from a 2.2 V to 5.5 V single supply; it can typically handle an output capacitor up to 1 nF and is fully specified on a load of 22 pF, therefore allowing easy usage as A/D converters input buffer.

1 Pin description

1.1 TSV791 single operational amplifier

Figure 1. Pin connections (top view)

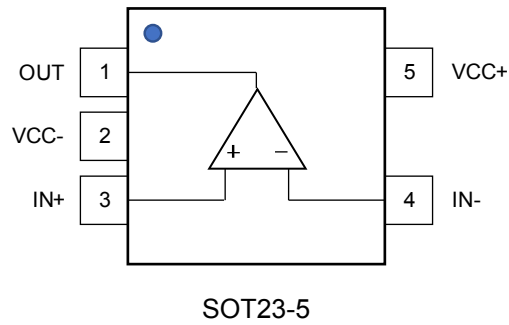
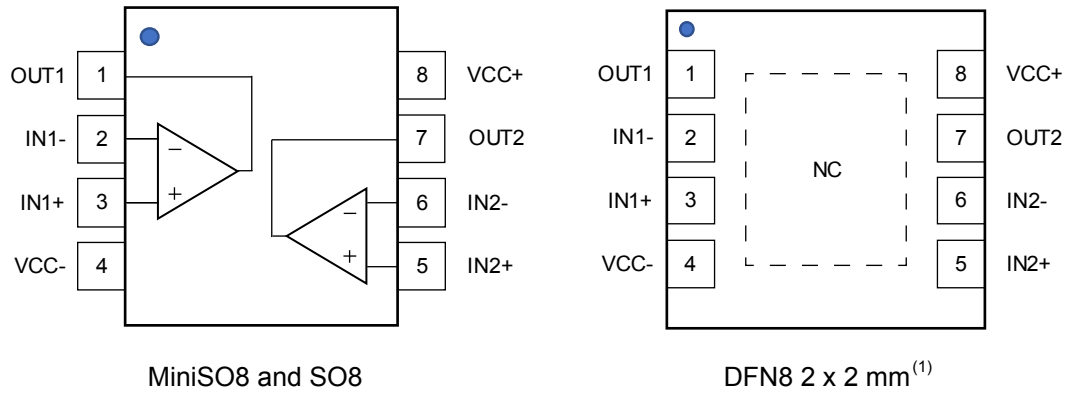


Table 1. Pin description

| Pin n° | Pin name | Description |
|--------|----------|-----------------------------|
| 1 | OUT | Output channel |
| 2 | VCC- | Negative supply voltage |
| 3 | IN+ | Non-inverting input channel |
| 4 | IN- | Inverting input channel |
| 5 | VCC+ | Positive supply voltage |

1.2 TSV792 dual operational amplifier

Figure 2. Pin connections (top view)



1. The exposed pad of the DFN8 2x2 can be connected to VCC- or left floating.

Table 2. Pin description

| Pin n° | Pin name | Description |
|--------|----------|-------------------------------|
| 1 | OUT1 | Output channel 1 |
| 2 | IN1- | Inverting input channel 1 |
| 3 | IN1+ | Non-inverting input channel 1 |
| 4 | VCC- | Negative supply voltage |
| 5 | IN2+ | Non-inverting input channel 2 |
| 6 | IN2- | Inverting input channel 2 |
| 7 | OUT2 | Output channel 2 |
| 8 | VCC+ | Positive supply voltage |

2 Absolute maximum ratings and operating conditions

Table 3. Absolute maximum ratings

| Symbol | Parameter ⁽¹⁾ | Value | Unit |
|----------------------------|---|--|--------|
| V_{CC} | Supply voltage | 6 | V |
| V_{id} | Input voltage differential ($V_{IN+} - V_{IN-}$) ⁽²⁾ | $\pm V_{CC}$ | V |
| V_{in} | Input voltage | $(V_{CC-}) - 0.2$ to $(V_{CC+}) + 0.2$ | V |
| I_{in} | Input current | ± 10 | mA |
| T_{stg} | Storage temperature | -65 to +150 | °C |
| T_j | Maximum junction temperature | 150 | °C |
| R_{th-ja} ⁽³⁾ | Thermal resistance junction-to-ambient | | °C / W |
| | SOT23-5 | 250 | |
| | DFN8 2x2 | 57 | |
| | MiniSO8 | 127 | |
| | SO8 | 125 | |
| ESD | HBM: human body model (industrial grade) ⁽⁴⁾ | 4 | kV |
| | HBM: human body model (automotive grade) ⁽⁵⁾ | 4 | kV |
| | CDM: charged device model ⁽⁶⁾ | 1 | kV |

1. All voltage values are with respect to the VCC- pin, unless otherwise specified.

2. The maximum input voltage differential value may be extended to the condition that the input current is limited to ± 10 mA.

3. R_{th-ja} is a typical value, obtained with PCB according to JEDEC 2s2p without vias.

4. Human body model: HBM test according to the standard ESDA-JS-001-2017.

5. Human body model: HBM test according to the standard AEC-Q100-002.

6. Charged device model: the CDM test is done according to the standard AEC-Q100-011.

Table 4. Operating conditions

| Symbol | Parameter | Value |
|------------|--------------------------------------|--|
| V_{CC} | Supply voltage | 2.2 V to 5.5 V |
| V_{icm} | Common mode input voltage range | $V_{CC-} - 0.1$ V to $V_{CC+} + 0.1$ V |
| T_{oper} | Operating free air temperature range | -40 °C to +125 °C |

3 Electrical characteristics

Table 5. Electrical characteristics at $V_{CC} = 5\text{ V}$, $V_{icm} = V_{OUT} = V_{CC} / 2$, $T = 25\text{ }^{\circ}\text{C}$, $R_L = 10\text{ k}\Omega$ connected to $V_{CC} / 2$ and $C_L = 22\text{ pF}$ (unless otherwise specified).

| Symbol | Parameter | Conditions | Min. | Typ. | Max. | Unit |
|--------------------------------|---|--|------|------|-----------|---------------------------------|
| DC performance | | | | | | |
| V_{io} | Input offset voltage | $T = 25\text{ }^{\circ}\text{C}$ | | | ± 200 | μV |
| | | $-40\text{ }^{\circ}\text{C} \leq T \leq 125\text{ }^{\circ}\text{C}$ | | | ± 700 | |
| $\Delta V_{io}/\Delta T$ | Input offset voltage temperature drift ⁽¹⁾ | $-40\text{ }^{\circ}\text{C} \leq T \leq 125\text{ }^{\circ}\text{C}$ | | | ± 5 | $\mu\text{V}/^{\circ}\text{C}$ |
| ΔV_{io} ⁽²⁾ | Input offset voltage long-term drift | $T = 25\text{ }^{\circ}\text{C}$ | | 750 | | $\text{nV}/\sqrt{\text{month}}$ |
| I_{ib} ⁽³⁾ | Input bias current | $T = 25\text{ }^{\circ}\text{C}$ | | 2 | | pA |
| | | $-40\text{ }^{\circ}\text{C} \leq T \leq 125\text{ }^{\circ}\text{C}$ | | 75 | | |
| I_{io} ⁽³⁾ | Input offset current | $T = 25\text{ }^{\circ}\text{C}$ | | 1 | | pA |
| | | $-40\text{ }^{\circ}\text{C} \leq T \leq 125\text{ }^{\circ}\text{C}$ | | 20 | | |
| A_{VD} | Open loop gain | $V_{CC-} + 200\text{ mV} \leq V_{OUT} \leq V_{CC+} - 200\text{ mV}$ $T = 25\text{ }^{\circ}\text{C}$ | 110 | 133 | | dB |
| | | $V_{CC-} + 200\text{ mV} \leq V_{OUT} \leq V_{CC+} - 200\text{ mV}$ $-40\text{ }^{\circ}\text{C} \leq T \leq 125\text{ }^{\circ}\text{C}$ | 90 | 113 | | |
| | | $R_L = 600\ \Omega$, $T = 25\text{ }^{\circ}\text{C}$ $V_{CC-} + 300\text{ mV} \leq V_{OUT} \leq V_{CC+} - 300\text{ mV}$ | 105 | 132 | | |
| | | $R_L = 600\ \Omega$, $-40\text{ }^{\circ}\text{C} \leq T \leq 125\text{ }^{\circ}\text{C}$ $V_{CC-} + 300\text{ mV} \leq V_{OUT} \leq V_{CC+} - 300\text{ mV}$ | 85 | | | |
| CMR1 | Common-mode rejection ratio | $V_{CC-} \leq V_{icm} \leq V_{CC+} - 2\text{ V}$, $T = 25\text{ }^{\circ}\text{C}$ | 100 | 120 | | dB |
| | | $V_{CC-} \leq V_{icm} \leq V_{CC+} - 2\text{ V}$, $-40\text{ }^{\circ}\text{C} \leq T \leq 125\text{ }^{\circ}\text{C}$ | 90 | 120 | | |
| CMR2 | $20 \cdot \log(\Delta V_{io}/\Delta V_{icm})$ | $V_{CC-} \leq V_{icm} \leq V_{CC+}$, $T = 25\text{ }^{\circ}\text{C}$ | 80 | 100 | | dB |
| | | $V_{CC-} \leq V_{icm} \leq V_{CC+}$, $-40\text{ }^{\circ}\text{C} \leq T \leq 125\text{ }^{\circ}\text{C}$ | 76 | 92 | | |
| SVR | Supply-voltage rejection ratio $20 \cdot \log(\Delta V_{io}/\Delta V_{CC})$ | $2.2\text{ V} \leq V_{CC} \leq 5.5\text{ V}$, $T = 25\text{ }^{\circ}\text{C}$, $V_{icm} = 0\text{ V}$ | 90 | 109 | | dB |
| | | $2.2\text{ V} \leq V_{CC} \leq 5.5\text{ V}$, $-40\text{ }^{\circ}\text{C} \leq T \leq 125\text{ }^{\circ}\text{C}$, $V_{icm} = 0\text{ V}$ | 90 | 108 | | |
| V_{OH} | High level output voltage drop ($V_{OH} = V_{CC+} - V_{OUT}$) | $T = 25\text{ }^{\circ}\text{C}$ | | | 20 | mV |
| | | $-40\text{ }^{\circ}\text{C} \leq T \leq 125\text{ }^{\circ}\text{C}$ | | | 25 | |
| V_{OL} | Low level output voltage drop ($V_{OL} = V_{OUT}$) | $T = 25\text{ }^{\circ}\text{C}$ | | | 10 | mV |
| | | $-40\text{ }^{\circ}\text{C} \leq T \leq 125\text{ }^{\circ}\text{C}$ | | | 15 | |
| I_{OUT} | I_{SINK} | OUT connected to V_{CC+} , $T = 25\text{ }^{\circ}\text{C}$ | 60 | 70 | | mA |
| | | OUT connected to V_{CC+} , $-40\text{ }^{\circ}\text{C} \leq T \leq 125\text{ }^{\circ}\text{C}$ | 35 | | | |
| | I_{SOURCE} | OUT connected to V_{CC-} , $T = 25\text{ }^{\circ}\text{C}$ | 50 | 60 | | |

| Symbol | Parameter | Conditions | Min. | Typ. | Max. | Unit |
|-----------------------|---|---|------|------|------|------------------------|
| I_{OUT} | I_{SOURCE} | OUT connected to V_{CC-} , $-40\text{ }^{\circ}\text{C} \leq T \leq 125\text{ }^{\circ}\text{C}$ | 40 | | | mA |
| I_{CC} | Supply current (by operational amplifier) | $T = 25\text{ }^{\circ}\text{C}$ | | 5.5 | 6 | mA |
| | | $-40\text{ }^{\circ}\text{C} \leq T \leq 125\text{ }^{\circ}\text{C}$ | | | 6 | |
| AC performance | | | | | | |
| GBP | Gain bandwidth product | $R_L = 10\text{ k}\Omega$, $C_L = 22\text{ pF}$ | 35 | 50 | | MHz |
| SR | Slew rate | $R_L = 10\text{ k}\Omega$, $C_L = 22\text{ pF}$, $A_V = 1\text{ V/V}$, 10 % to 90 % | | 30 | | V/ μs |
| CR | Cross talk | $V_{OUT} = 4\text{ V}_{pp}$, $R_L = 10\text{ k}\Omega$, $A_V = +101$, $f = 1\text{ kHz}$ | | 126 | | dB |
| Φ_m | Phase margin | $R_L = 10\text{ k}\Omega$ | | 53 | | degrees |
| e_n | Input voltage noise density | $f = 10\text{ Hz}$ | | 140 | | nV/ $\sqrt{\text{Hz}}$ |
| | | $f = 100\text{ Hz}$ | | 43 | | |
| | | $f = 10\text{ kHz}$ | | 6.5 | | |
| $e_n\text{ p-p}$ | Input noise voltage | $0.1\text{ Hz} \leq f \leq 10\text{ Hz}$ | | 9 | | μV_{pp} |
| C_{in} | Input capacitance | Differential | | 6.3 | | pF |
| | | Common mode | | 1.6 | | |

1. See Section 5.2 *Input offset voltage drift overtemperature.*
2. See Section 5.3 *Long term input offset voltage drift.*
3. *Guaranteed by characterization.*

Table 6. Electrical characteristics at $V_{CC} = 3.3\text{ V}$, $V_{icm} = V_{OUT} = V_{CC} / 2$, $T = 25\text{ °C}$, $R_L = 10\text{ k}\Omega$ connected to $V_{CC} / 2$ and $C_L = 22\text{ pF}$ (unless otherwise specified).

| Symbol | Parameter | Conditions | Min. | Typ. | Max. | Unit |
|---|---|--|------|------|-----------|-------------------------|
| DC performance | | | | | | |
| V_{io} | Input offset voltage | $V_{icm} = 0\text{ V}$, $T = 25\text{ °C}$ | | | ± 200 | μV |
| | | $V_{icm} = 0\text{ V}$, $-40\text{ °C} \leq T \leq 125\text{ °C}$ | | | ± 700 | |
| $\Delta V_{io}/\Delta T$ ⁽¹⁾ | Input offset voltage temperature drift | $V_{icm} = 0\text{ V}$, $-40\text{ °C} \leq T \leq 125\text{ °C}$ | | | ± 5 | $\mu\text{V}/\text{°C}$ |
| I_{ib} ⁽²⁾ | Input bias current | $T = 25\text{ °C}$ | | 1.5 | | pA |
| | | $-40\text{ °C} \leq T \leq 125\text{ °C}$ | | 60 | | |
| I_{io} ⁽²⁾ | Input offset current | $T = 25\text{ °C}$ | | 1 | | pA |
| | | $-40\text{ °C} \leq T \leq 125\text{ °C}$ | | 20 | | |
| A_{VD} | Open loop gain | $V_{CC-} + 200\text{ mV} \leq V_{OUT} \leq V_{CC+} - 200\text{ mV}$, $T = 25\text{ °C}$ | 105 | 130 | | dB |
| | | $V_{CC-} - 200\text{ mV} \leq V_{OUT} \leq V_{CC+} - 200\text{ mV}$, $-40\text{ °C} \leq T \leq 125\text{ °C}$ | 90 | 113 | | |
| | | $R_L = 600\ \Omega$, $T = 25\text{ °C}$ | 100 | 129 | | |
| | | $V_{CC-} + 300\text{ mV} \leq V_{OUT} \leq V_{CC+} - 300\text{ mV}$, $R_L = 600\ \Omega$, $-40\text{ °C} \leq T \leq 125\text{ °C}$ | 85 | 99 | | |
| | | $V_{CC-} + 300\text{ mV} \leq V_{OUT} \leq V_{CC+} - 300\text{ mV}$ | | | | |
| CMR1 | Common-mode rejection ratio $20 \cdot \log(\Delta V_{io}/\Delta V_{icm})$ | $V_{CC-} \leq V_{icm} \leq V_{CC+} - 2\text{ V}$, $T = 25\text{ °C}$ | 95 | 116 | | dB |
| | | $V_{CC-} \leq V_{icm} \leq V_{CC+} - 2\text{ V}$, $-40\text{ °C} \leq T \leq 125\text{ °C}$ | 85 | 111 | | |
| CMR2 | | $V_{CC-} \leq V_{icm} \leq V_{CC+}$, $T = 25\text{ °C}$ | 77 | 97 | | dB |
| | | $V_{CC-} \leq V_{icm} \leq V_{CC+}$, $-40\text{ °C} \leq T \leq 125\text{ °C}$ | 70 | 90 | | |
| V_{OH} | High level output voltage drop ($V_{OH} = V_{CC+} - V_{OUT}$) | $T = 25\text{ °C}$ | | | 25 | mV |
| | | $-40\text{ °C} \leq T \leq 125\text{ °C}$ | | | 40 | |
| V_{OL} | Low level output voltage drop ($V_{OL} = V_{OUT}$) | $T = 25\text{ °C}$ | | | 15 | mV |
| | | $-40\text{ °C} \leq T \leq 125\text{ °C}$ | | | 30 | |
| I_{OUT} | I_{SINK} | OUT connected to V_{CC+} , $T = 25\text{ °C}$ | 55 | 63 | | mA |
| | | OUT connected to V_{CC+} , $-40\text{ °C} \leq T \leq 125\text{ °C}$ | 35 | | | |
| | I_{SOURCE} | OUT connected to V_{CC-} , $T = 25\text{ °C}$ | 50 | 63 | | |
| | | OUT connected to V_{CC-} , $-40\text{ °C} \leq T \leq 125\text{ °C}$ | 35 | | | |
| I_{CC} | Supply current (by operational amplifier) | $T = 25\text{ °C}$ | | 5.3 | 5.8 | mA |
| | | $-40\text{ °C} \leq T \leq 125\text{ °C}$ | | | 5.8 | |
| AC performance | | | | | | |
| GBP | Gain bandwidth product | $R_L = 10\text{ k}\Omega$, $C_L = 22\text{ pF}$ | 35 | 50 | | MHz |

| Symbol | Parameter | Conditions | Min. | Typ. | Max. | Unit |
|----------|-----------------------------|--|------|------|------|------------------------|
| SR | Slew rate | $R_L = 10\text{ k}\Omega$, $C_L = 22\text{ pF}$, $A_V = 1\text{ V/V}$, 10 % to 90 % | | 30 | | V/ μ s |
| CR | Cross talk | $V_{OUT} = 4\text{ V}_{pp}$, $R_L = 10\text{ k}\Omega$, $A_V = +101$, $f = 1\text{ kHz}$ | | 126 | | dB |
| Φ_m | Phase margin | $R_L = 10\text{ k}\Omega$ | | 53 | | degrees |
| en | Input voltage noise density | $f = 10\text{ Hz}$ | | 140 | | nV/ $\sqrt{\text{Hz}}$ |
| | | $f = 100\text{ Hz}$ | | 43 | | |
| | | $f = 10\text{ kHz}$ | | 6.5 | | |
| C_{in} | Input capacitance | Differential | | 6.3 | | pF |
| | | Common mode | | 1.6 | | |

1. See Section 5.2 *Input offset voltage drift overtemperature*.
2. Guaranteed by characterization.

Table 7. Electrical characteristics at $V_{CC} = 2.2\text{ V}$, $V_{icm} = V_{OUT} = V_{CC} / 2$, $T = 25\text{ }^\circ\text{C}$, $R_L = 10\text{ k}\Omega$ connected to $V_{CC} / 2$ and $C_L = 22\text{ pF}$ (unless otherwise specified).

| Symbol | Parameter | Conditions | Min. | Typ. | Max. | Unit |
|---|---|---|------|----------|-----------|------------------------------|
| DC performance | | | | | | |
| V_{io} | Input offset voltage | $V_{icm} = 0\text{ V}$, $T = 25\text{ }^\circ\text{C}$ | | ± 50 | ± 200 | μV |
| | | $V_{icm} = 0\text{ V}$, $-40\text{ }^\circ\text{C} \leq T \leq 125\text{ }^\circ\text{C}$ | | | ± 700 | |
| $\Delta V_{io}/\Delta T$ ⁽¹⁾ | Input offset voltage temperature drift | $V_{icm} = 0\text{ V}$, $-40\text{ }^\circ\text{C} \leq T \leq 125\text{ }^\circ\text{C}$ | | | ± 5 | $\mu\text{V}/^\circ\text{C}$ |
| I_{ib} ⁽²⁾ | Input bias current | $T = 25\text{ }^\circ\text{C}$ | | 1 | | pA |
| | | $-40\text{ }^\circ\text{C} \leq T \leq 125\text{ }^\circ\text{C}$ | | 45 | | |
| I_{io} ⁽²⁾ | Input offset current | $T = 25\text{ }^\circ\text{C}$ | | 1 | | pA |
| | | $-40\text{ }^\circ\text{C} \leq T \leq 125\text{ }^\circ\text{C}$ | | 13 | | |
| A_{VD} | Open loop gain | $V_{CC-} + 200\text{ mV} \leq V_{OUT} \leq V_{CC+} - 200\text{ mV}$, $T = 25\text{ }^\circ\text{C}$ | 95 | 120 | | dB |
| | | $V_{CC-} - 200\text{ mV} \leq V_{OUT} \leq V_{CC+} - 200\text{ mV}$, $-40\text{ }^\circ\text{C} \leq T \leq 125\text{ }^\circ\text{C}$ | 85 | 107 | | |
| | | $R_L = 600\ \Omega$, $V_{CC-} + 300\text{ mV} \leq V_{OUT} \leq V_{CC+} - 300\text{ mV}$, $T = 25\text{ }^\circ\text{C}$ | 90 | 119 | | |
| | | $R_L = 600\ \Omega$, $V_{CC-} - 300\text{ mV} \leq V_{OUT} \leq V_{CC+} - 300\text{ mV}$, $-40\text{ }^\circ\text{C} \leq T \leq 125\text{ }^\circ\text{C}$ | 80 | 99 | | |
| CMR | Common-mode rejection ratio $20.\log(\Delta V_{io}/\Delta V_{icm})$ | $V_{CC-} \leq V_{icm} \leq V_{CC+}$, $T = 25\text{ }^\circ\text{C}$ | 73 | 94 | | dB |
| | | $V_{CC-} \leq V_{icm} \leq V_{CC+}$, $-40\text{ }^\circ\text{C} \leq T \leq 125\text{ }^\circ\text{C}$ | 67 | 85 | | |
| V_{OH} | High level output voltage drop ($V_{OH} = V_{CC+} - V_{OUT}$) | $T = 25\text{ }^\circ\text{C}$ | | | 25 | mV |
| | | $-40\text{ }^\circ\text{C} \leq T \leq 125\text{ }^\circ\text{C}$ | | | 40 | |
| V_{OL} | Low level output voltage drop ($V_{OL} = V_{OUT}$) | $T = 25\text{ }^\circ\text{C}$ | | | 15 | mV |
| | | $-40\text{ }^\circ\text{C} \leq T \leq 125\text{ }^\circ\text{C}$ | | | 30 | |
| I_{OUT} | I_{SINK} | OUT connected to V_{CC+} , $T = 25\text{ }^\circ\text{C}$ | 55 | 62 | | mA |
| | | OUT connected to V_{CC+} , $-40\text{ }^\circ\text{C} \leq T \leq 125\text{ }^\circ\text{C}$ | 35 | | | |
| | I_{SOURCE} | OUT connected to V_{CC-} , $T = 25\text{ }^\circ\text{C}$ | 50 | 62 | | |
| | | OUT connected to V_{CC-} , $-40\text{ }^\circ\text{C} \leq T \leq 125\text{ }^\circ\text{C}$ | 35 | | | |
| I_{CC} | Supply current (by operational amplifier) | $V_{icm} = 0\text{ V}$, $T = 25\text{ }^\circ\text{C}$ | | 5 | 5.5 | mA |
| | | $V_{icm} = 0\text{ V}$, $-40\text{ }^\circ\text{C} \leq T \leq 125\text{ }^\circ\text{C}$ | | | 5.5 | |
| AC performance | | | | | | |
| GBP | Gain bandwidth product | $R_L = 10\text{ k}\Omega$ | 35 | 50 | | MHz |
| SR | Slew rate | $R_L = 10\text{ k}\Omega$, $A_V = 1\text{ V/V}$, 10 % to 90 % | | 30 | | $\text{V}/\mu\text{s}$ |
| CR | Cross talk | $V_{OUT} = 4\text{ V}_{pp}$, $R_L = 10\text{ k}\Omega$, $A_V = +101$, $f = 1\text{ kHz}$ | | 126 | | dB |

| Symbol | Parameter | Conditions | Min. | Typ. | Max. | Unit |
|----------|-----------------------------|---------------------------|------|------|------|------------------------------|
| Φ_m | Phase margin | $R_L = 10\text{ k}\Omega$ | | 69 | | degrees |
| e_n | Input voltage noise density | $f = 10\text{ Hz}$ | | 250 | | $\text{nV}/\sqrt{\text{Hz}}$ |
| | | $f = 100\text{ Hz}$ | | 94 | | |
| | | $f = 10\text{ kHz}$ | | 15 | | |
| C_{in} | Input capacitance | Differential | | 6.3 | | pF |
| | | Common mode | | 1.6 | | |

1. See Section 5.2 *Input offset voltage drift overtemperature*.
2. *Guaranteed by characterization*.

4 Typical performance characteristics

$R_L = 10\text{ k}\Omega$ connected to $V_{CC} / 2$ and $C_L = 22\text{ pF}$, unless otherwise specified.

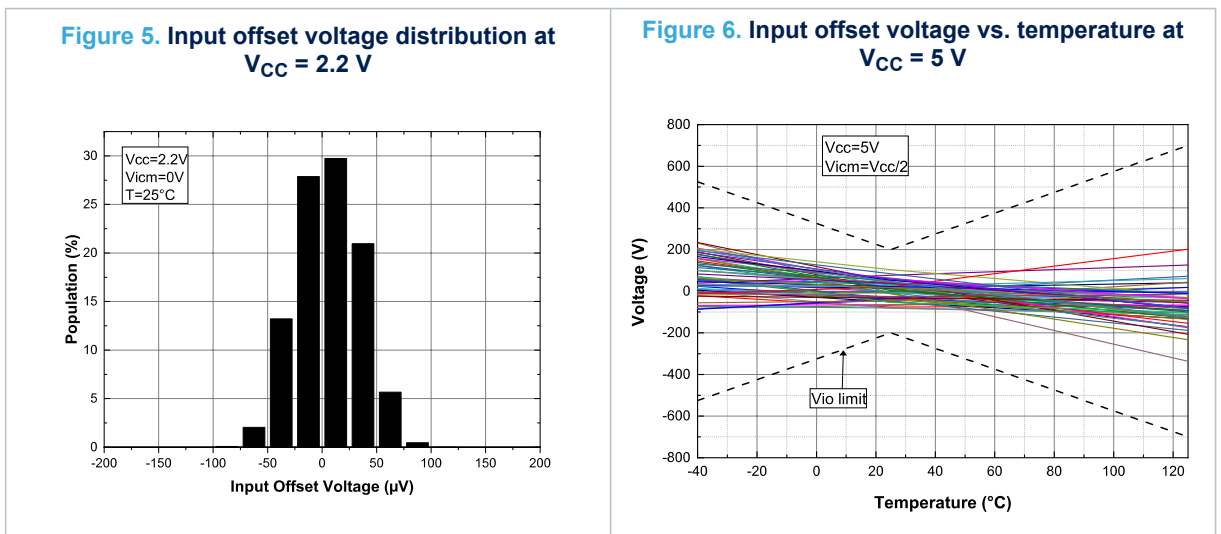
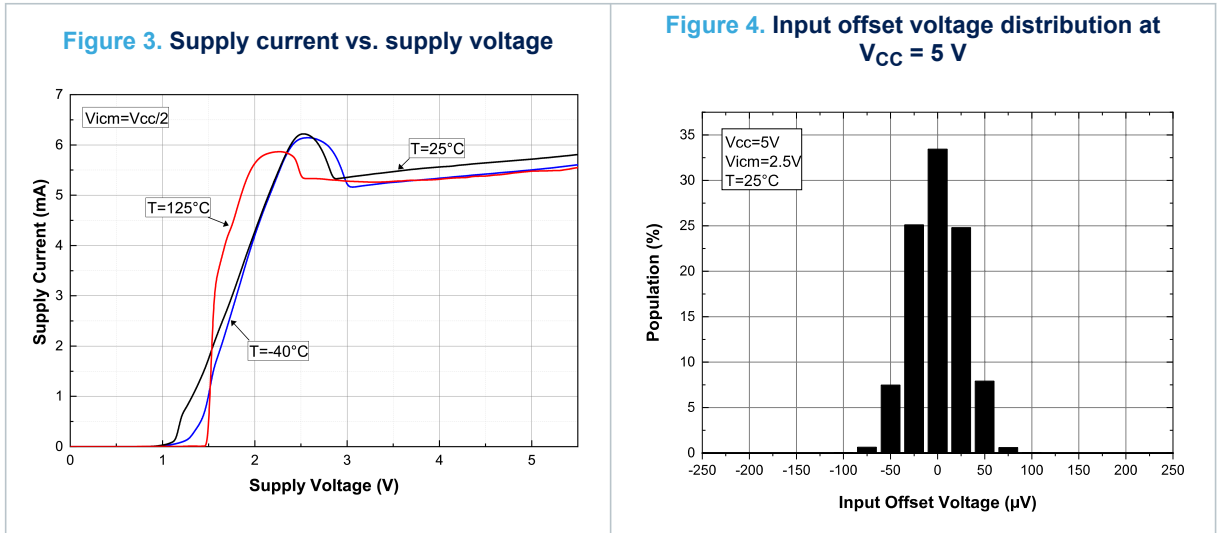


Figure 7. Input offset voltage vs. temperature at $V_{CC} = 2.2\text{ V}$

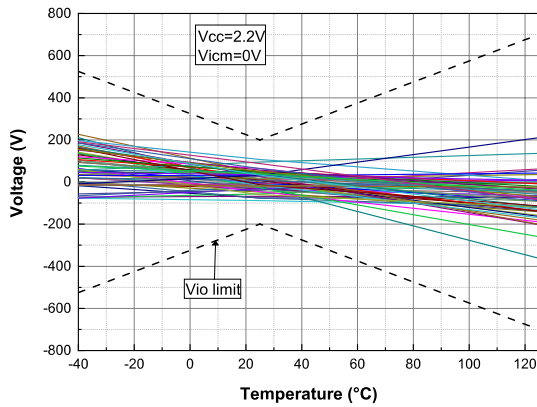


Figure 8. Input offset voltage thermal coefficient distribution at $V_{CC} = 5\text{ V}$

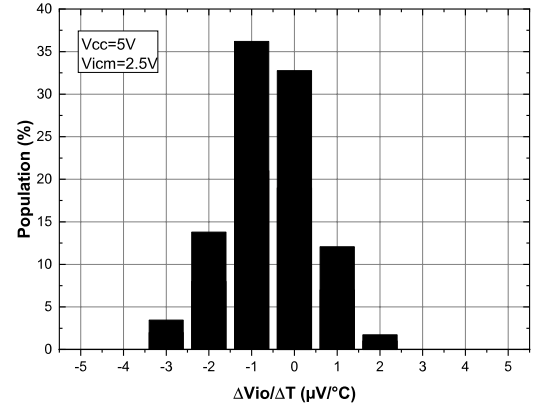


Figure 9. Input offset voltage thermal coefficient at $V_{CC} = 2.2\text{ V}$

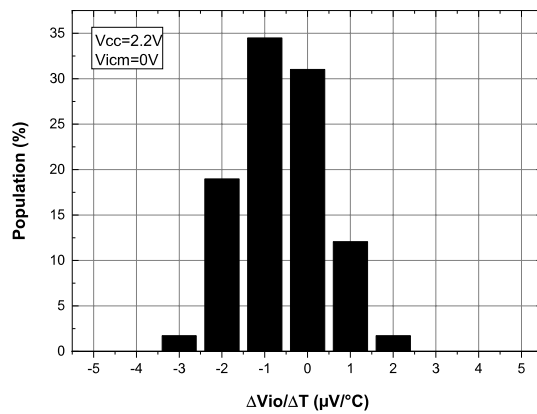


Figure 10. Input offset voltage vs. supply voltage

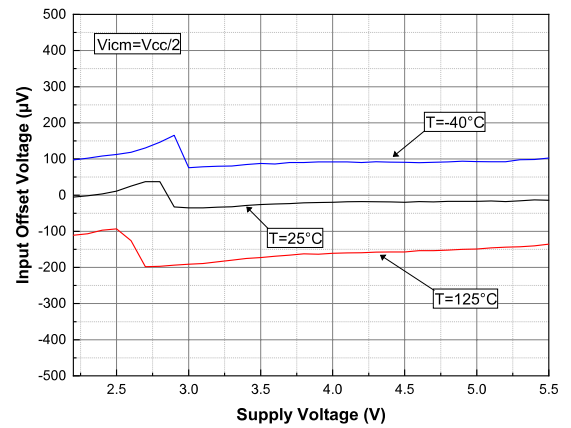


Figure 11. Input offset voltage vs. common mode voltage at $V_{CC} = 5\text{ V}$

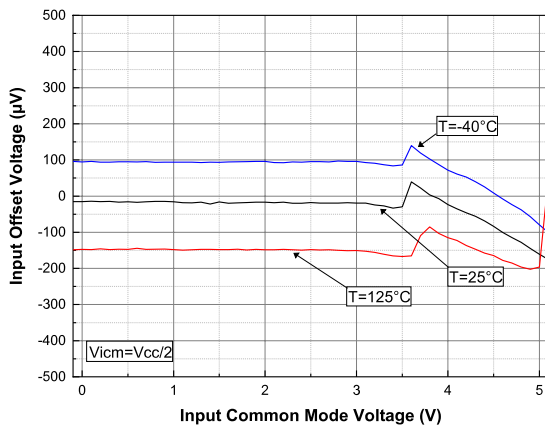


Figure 12. Input offset voltage vs. common mode voltage at $V_{CC} = 2.2\text{ V}$

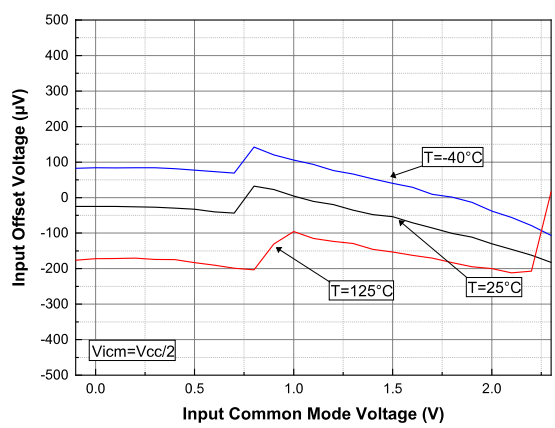


Figure 13. Input bias current vs. temperature at $V_{icm} = V_{CC} / 2$

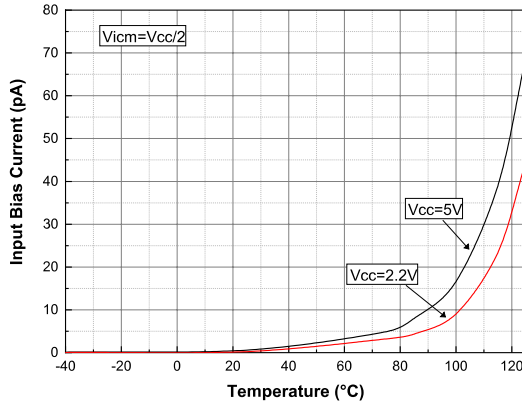


Figure 14. Input bias current vs. common mode voltage at $V_{CC} = 5 V$

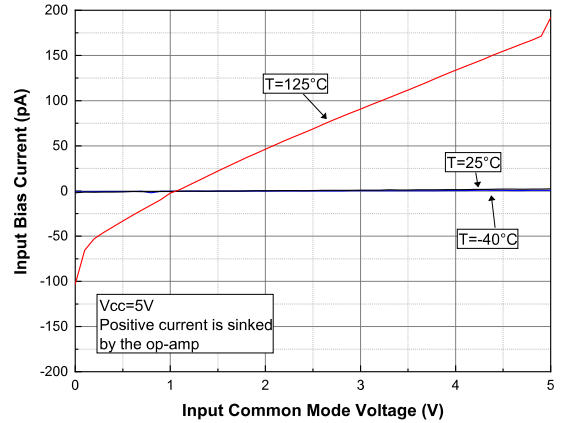


Figure 15. Output current vs. output voltage at $V_{CC} = 5 V$

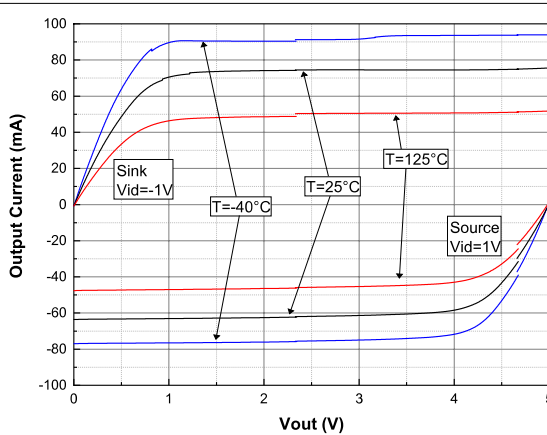


Figure 16. Output current vs. output voltage at $V_{CC} = 2.2 V$

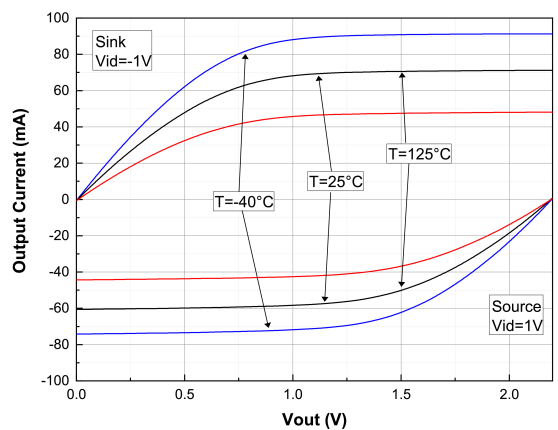


Figure 17. Output saturation voltage (V_{OL}) vs. supply voltage

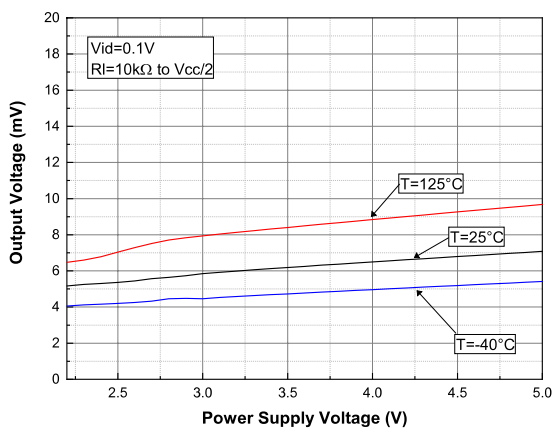


Figure 18. Output saturation voltage (V_{OH}) vs. supply voltage

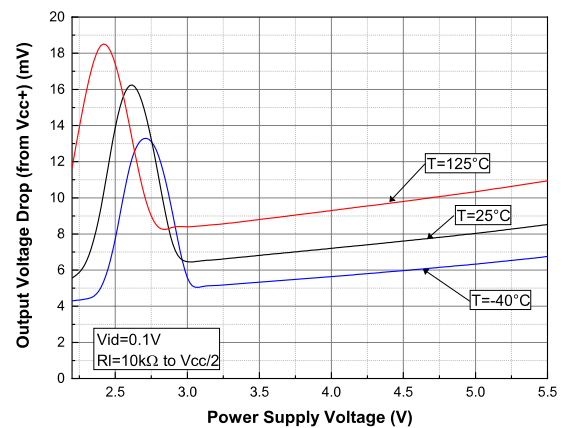


Figure 19. Positive slew rate at $V_{CC} = 5\text{ V}$

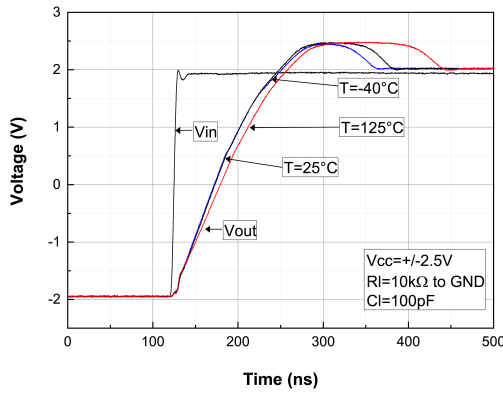


Figure 20. Negative slew rate at $V_{CC} = 5\text{ V}$

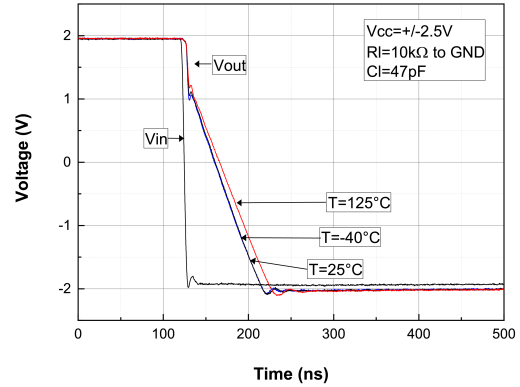


Figure 21. Slew rate vs. V_{CC}

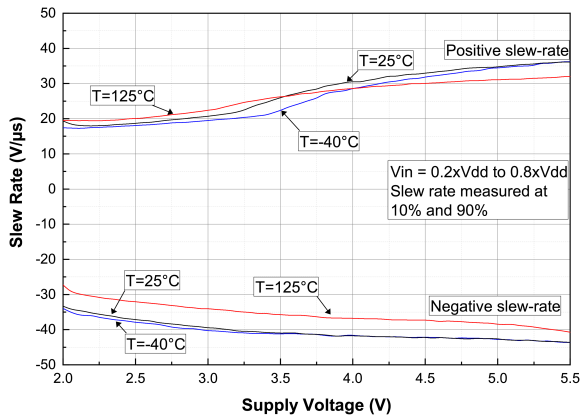


Figure 22. Open loop bode diagram at $V_{CC} = 5\text{ V}$

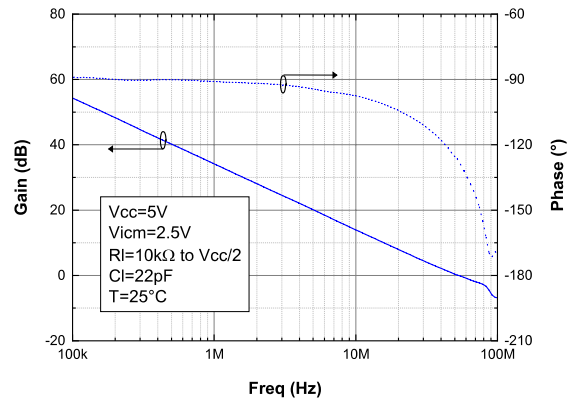


Figure 23. Open loop bode diagram at $V_{CC} = 2.2\text{ V}$

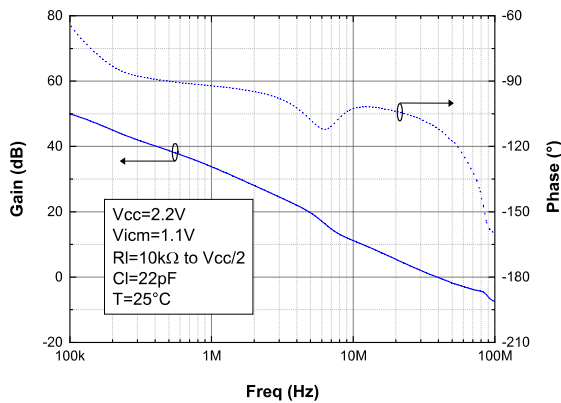


Figure 24. Closed loop bode diagram at $V_{CC} = 5\text{ V}$

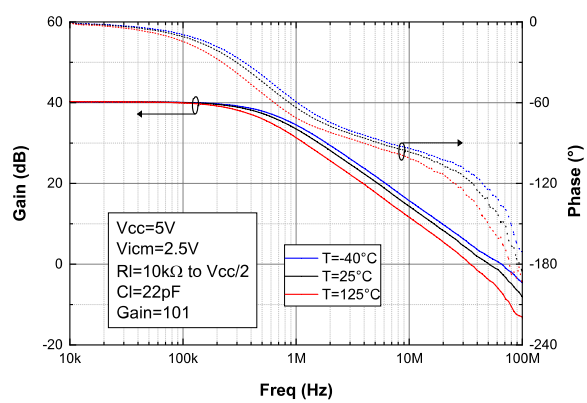


Figure 25. Closed loop bode diagram at $V_{CC} = 2.2\text{ V}$

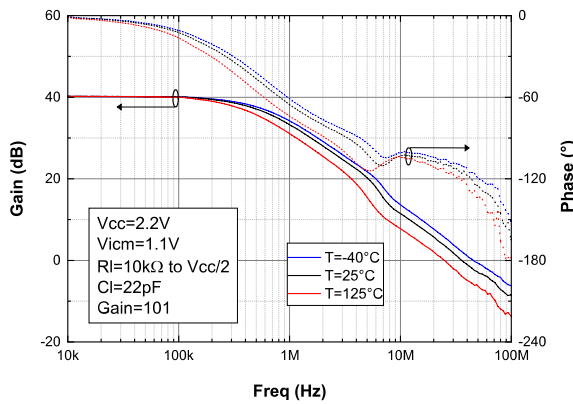


Figure 26. Phase margin vs. common mode voltage and load current at $V_{CC} = 5\text{ V}$

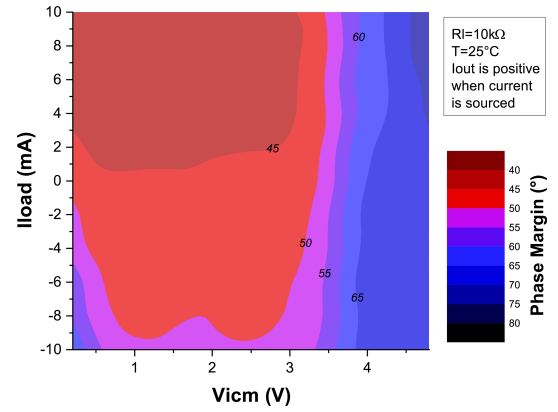


Figure 27. Phase margin vs. capacitive load

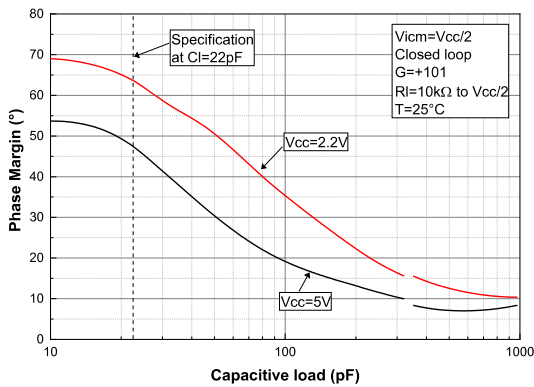


Figure 28. Small step response at $V_{CC} = 5\text{ V}$

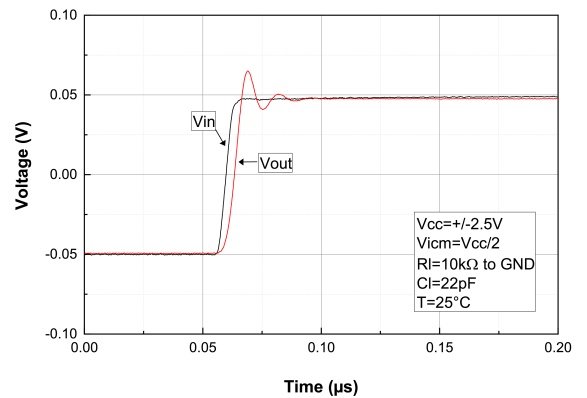


Figure 29. Small step response at $V_{CC} = 2.2\text{ V}$

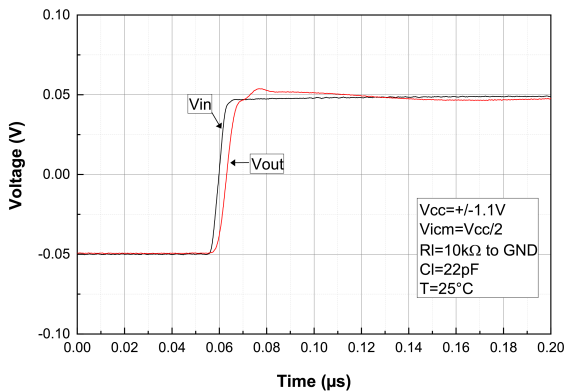


Figure 30. Desaturation from low rail at $V_{CC} = 5\text{ V}$

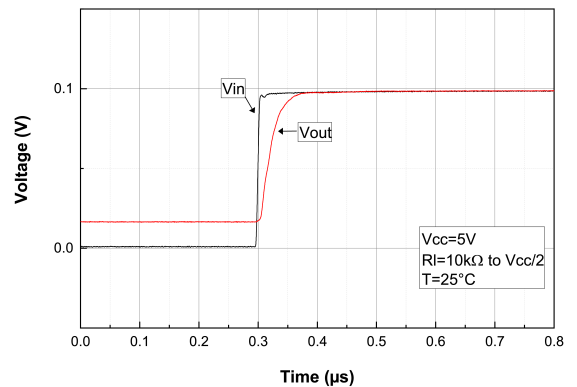


Figure 31. Desaturation from high rail at $V_{CC} = 5\text{ V}$

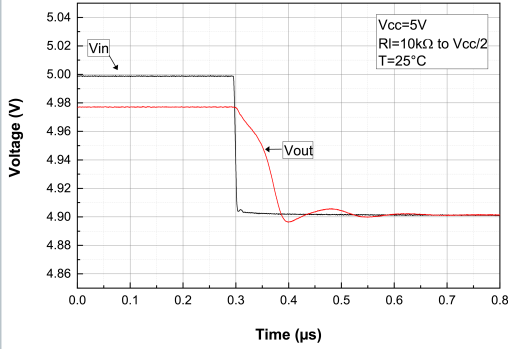


Figure 32. Settling time output high to low at $V_{CC} = 5\text{ V}$

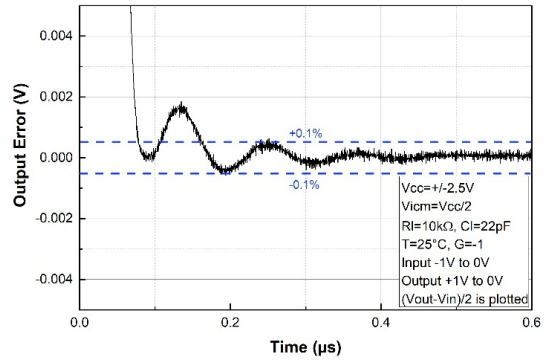


Figure 33. Settling time output low to high at $V_{CC} = 5\text{ V}$

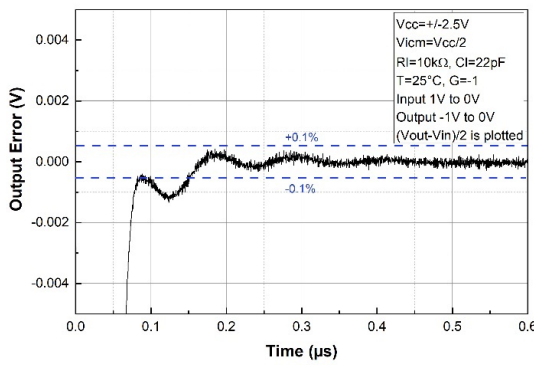


Figure 34. Settling time output high to low at $V_{CC} = 2.2\text{ V}$

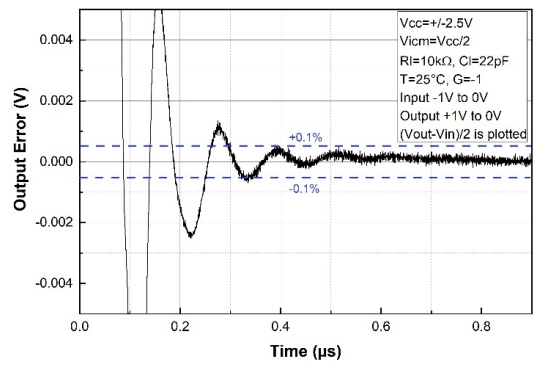


Figure 35. Settling time output low to high at $V_{CC} = 2.2\text{ V}$

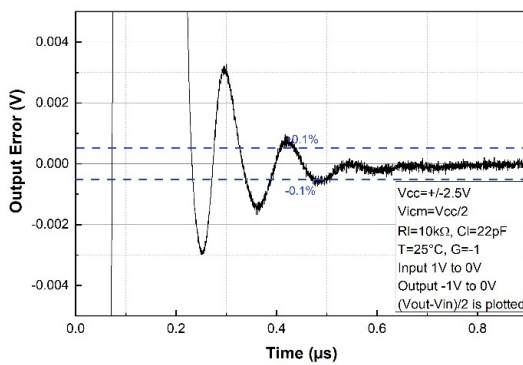


Figure 36. Small step overshoot vs. load capacitance

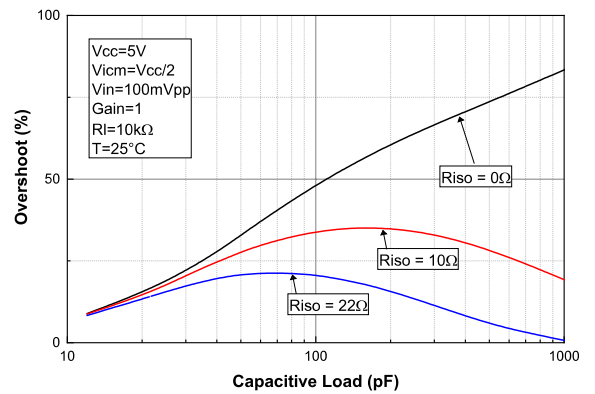


Figure 37. Linearity vs. load resistance at $V_{CC} = 5\text{ V}$

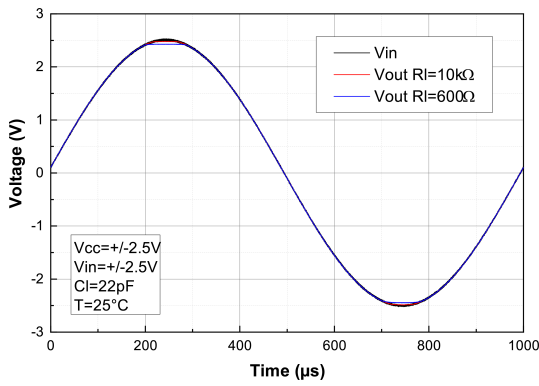


Figure 38. Noise vs. frequency

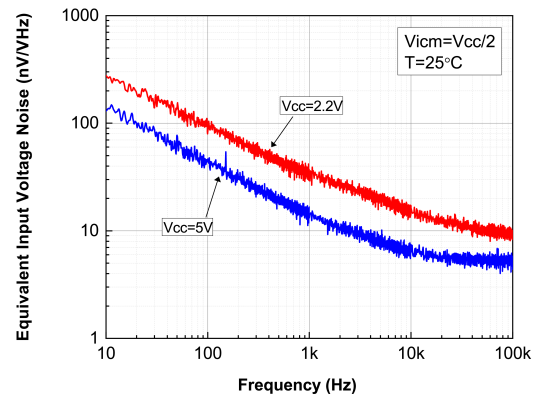


Figure 39. Noise vs. time at $V_{CC} = 5\text{ V}$

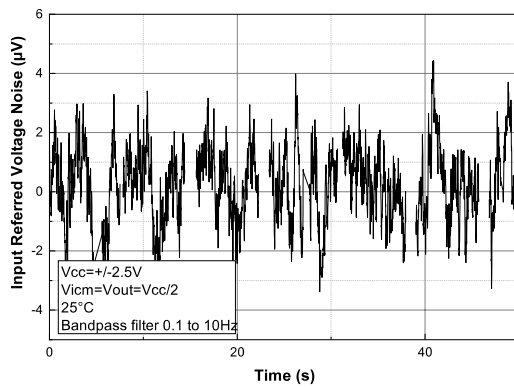


Figure 40. THD+N vs. frequency

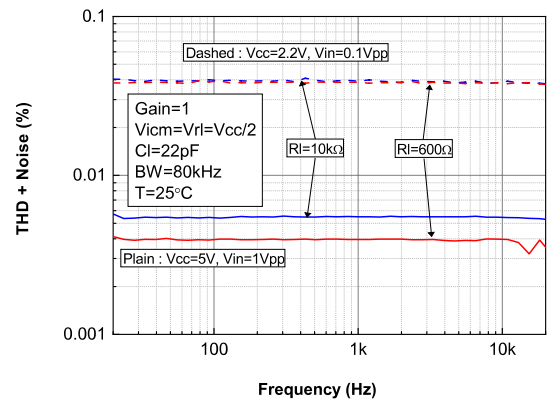


Figure 41. THD+N vs. output voltage

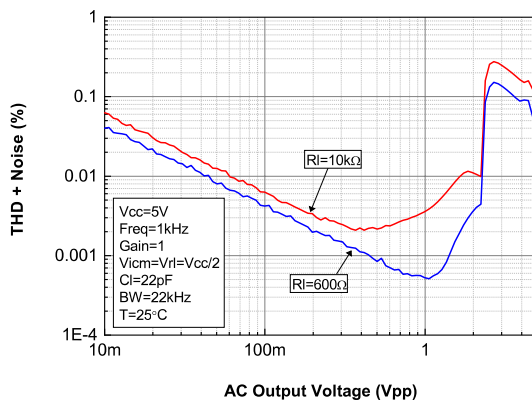


Figure 42. CMRR vs. frequency at $V_{CC} = 5\text{ V}$

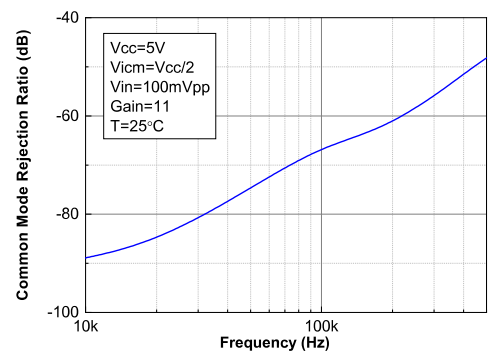


Figure 43. PSRR vs. frequency at $V_{CC} = 5\text{ V}$

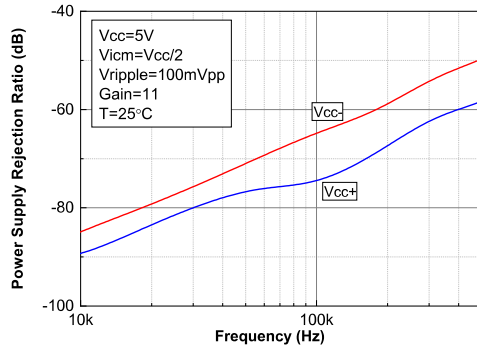
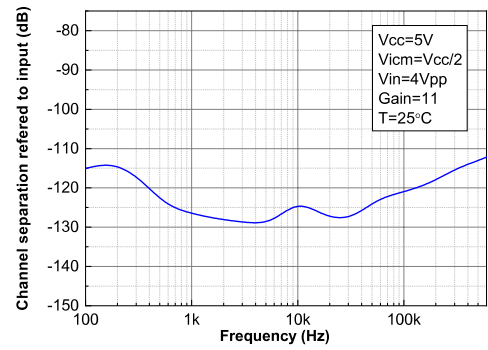


Figure 44. Crosstalk vs. frequency at $V_{CC} = 5\text{ V}$



5 Application information

5.1 Operating voltages

The TSV79x devices can operate from 2.2 to 5.5 V. The parameters are fully specified at 2.2 V, 3.3 V and 5 V power supplies. However, the parameters are very stable over the full V_{CC} range and several characterization curves show the TSV79x device characteristics over the full operating range. Additionally, the main specifications are guaranteed in extended temperature range from -40 to 125 °C.

The TSV79X devices are rail-to-rail input and output, and feature two input transistor pairs, allowing the op-amp to operate over all the common mode range, from $V_{CC-} - 0.1$ V, to $V_{CC+} + 0.1$ V. The input pair transition typically occurs at $V_{CC+} - 1.4$ V, as seen in figures 11 and 12. The precision and dynamic performances are particularly optimized on the low pair, from $V_{CC-} - 0.1$ V to $V_{CC+} - 2$ V, and operating in this V_{icm} range is advised for best performance whenever possible. Also, operating near the pair transition should be avoided when precision is a concern, as CMRR can be lower in these conditions.

5.2 Input offset voltage drift overtemperature

The maximum input voltage drift variation overtemperature is defined as the offset variation related to the offset value measured at 25 °C. The operational amplifier is one of the main circuits of the signal conditioning chain, and the amplifier input offset (V_{io}) is a major contributor to the chain accuracy.

The signal chain accuracy at 25 °C can be compensated during production at application level. The maximum input voltage drift overtemperature enables the system designer to anticipate the effect of temperature variations. The maximum input voltage drift overtemperature is computed using Equation 1.

$$\frac{\Delta V_{io}}{\Delta T} = \max \left| \frac{V_{io}(T) - V_{io}(25^{\circ}\text{C})}{T - 25^{\circ}\text{C}} \right|_{T = -40^{\circ}\text{C and } T = 125^{\circ}\text{C}} \quad (1)$$

The datasheet maximum value is guaranteed by a measurement on a representative sample size ensuring a C_{pk} (process capability index) greater than 1.3.

5.3 Long term input offset voltage drift

To evaluate product reliability, two types of stress acceleration are used:

- Voltage acceleration, by changing the applied voltage
- Temperature acceleration, by changing the die temperature (below the maximum junction temperature allowed by the technology) with the ambient temperature.

The voltage acceleration has been defined based on JEDEC results, and is defined using Equation 2

$$A_{FV} = e^{\beta \cdot (V_S - V_U)} \quad (2)$$

Where:

A_{FV} is the voltage acceleration factor

β is the voltage acceleration constant in $1/V$, constant technology parameter ($\beta = 1$)

V_S is the stress voltage used for the accelerated test

V_U is the voltage used for the application

The temperature acceleration is driven by the Arrhenius model, and is defined in Equation 3.

$$A_{FT} = e^{\frac{E_a}{k} \cdot \left(\frac{1}{T_U} - \frac{1}{T_S} \right)} \quad (3)$$

Where:

A_{FT} is the temperature acceleration factor

E_a is the activation energy of the technology based on the failure rate

k is the Boltzmann constant (8.6173×10^{-5} eV . K⁻¹)

T_U is the temperature of the die when V_U is used (K)

T_S is the temperature of the die under temperature stress (K)

The final acceleration factor, A_F , is the multiplication of the voltage acceleration factor and the temperature acceleration factor (Equation 4).

$$A_F = A_{FT} \cdot A_{FV} \quad (4)$$

A_F is calculated using the temperature and voltage defined in the mission profile of the product. The A_F value can then be used in Equation x to calculate the number of months of use equivalent to 1000 hours of reliable stress duration.

$$\text{Months} = A_F \times 1000 \text{ h} \times 12 \text{ months} / (24 \text{ h} \times 365.25 \text{ days})$$

To evaluate the op-amp reliability, a follower stress condition is used where V_{CC} is defined as a function of the maximum operating voltage and the absolute maximum rating (as recommended by JEDEC rules). The V_{io} drift (in μV) of the product after 1000 h of stress is tracked with parameters at different measurement conditions (see Equation 5).

$$V_{CC} = \max(V_{op}) \text{ with } V_{icm} = \frac{V_{CC}}{2} \quad (5)$$

The long term drift parameter ΔV_{io} (in $\mu\text{V} \cdot \text{month}^{-1/2}$), estimating the reliability performance of the product, is obtained using the ratio of the V_{io} (input offset voltage value) drift over the square root of the calculated number of months (Equation 6).

$$\Delta V_{io} = \frac{V_{io \text{ drift}}}{\sqrt{\text{months}}} \quad (6)$$

Where V_{io} drift is the measured drift value in the specified test conditions after 1000 h stress duration.

The V_{io} final drift, in μV , to be measured on the device in real operation conditions can be computed from Equation 7.

$$V_{io \text{ final drift}}(t_{op}, T_{op}, V_{CC}) = \Delta V_{io} \cdot \sqrt{t_{op} \cdot e^{\beta \cdot (V_{CC} - V_{CC \text{ nom}})} \cdot e^{\frac{E_a}{k} \cdot \left(\frac{1}{297} - \frac{1}{T_{op}} \right)}} \quad (7)$$

Where:

ΔV_{io} is the long term drift parameter in $\mu\text{V} \cdot \sqrt{\text{month}}$

t_{op} is the operating time seen by the device, in months

T_{op} is the operating temperature

V_{CC} is the power supply during operating time

$V_{CC \text{ nom}}$ is the nominal V_{CC} at which the ΔV_{io} is computed (5 V for TSV79x)

E_a is the activation energy of the technology (here 0.7 eV).

5.4 Unused channel

When one of the two channels of the TSV792 is not used, it must be properly connected in order to avoid internal oscillations that can negatively impact the signal integrity on the other channel, as well as the current consumption. Two different configurations can be used:

Gain configuration: the channel can be set in gain, the input can be set to any voltage within the V_{icm} operating range.

Comparator configuration: the channel can be set to a comparator configuration (without negative feedback). In this case, positive and negative inputs can be set to any value provided these values are significantly different (100 mV or more, to avoid oscillation between positive and negative state).

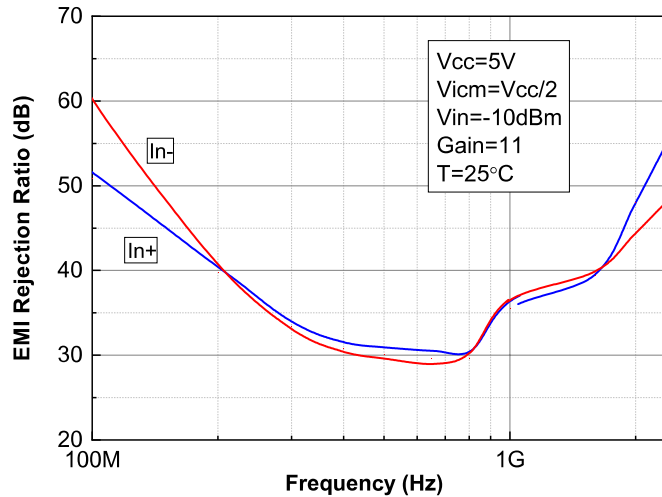
5.5 EMI rejection

The electromagnetic interference (EMI) rejection ratio, or EMIRR, describes the EMI immunity of operational amplifiers. An adverse effect that is common to many op-amps is a change in the offset voltage as a result of RF signal rectification. EMIRR is defined in Equation 8:

$$EMIRR = 20 \cdot \log\left(\frac{V_{in \text{ pp}}}{\Delta V_{io}}\right) \quad (8)$$

The TSV79x has been specially designed to minimize susceptibility to EMIRR and shows a low sensitivity. As seen in Figure 45, EMI rejection ratio has been measured on both inputs and output, from 400 MHz to 2.4 GHz.

Figure 45. EMIRR on IN+ and IN- pins



EMIRR performances might be improved by adding small capacitances (in the pF range) on the inputs, power supply and output pins. These capacitances help to minimize the impedance of these nodes at high frequencies.

5.6 Maximum power dissipation

The usable output load current drive is limited by the maximum power dissipation allowed by the device package. The absolute maximum junction temperature for the TSV79x is 150 °C. The junction temperature can be estimated as follows:

$$T_J = P_D \times \theta_{JA} + T_A \quad (9)$$

T_J is the die junction temperature

P_D is the power dissipated in the package

θ_{JA} is the junction to ambient thermal resistance of the package.

T_A is the ambient temperature.

The power dissipated in the package P_D is the sum of the quiescent power dissipated and the power dissipated by the output stage transistor. It is calculated as follows:

$$P_D = (V_{CC} \times I_{CC}) + (V_{CC} + V_{OUT}) \times I_{Load} \text{ when the op-amp is sourcing the current.}$$

$$P_D = (V_{CC} \times I_{CC}) + (V_{OUT} - V_{CC-}) \times I_{Load} \text{ when the op-amp is sinking the current.}$$

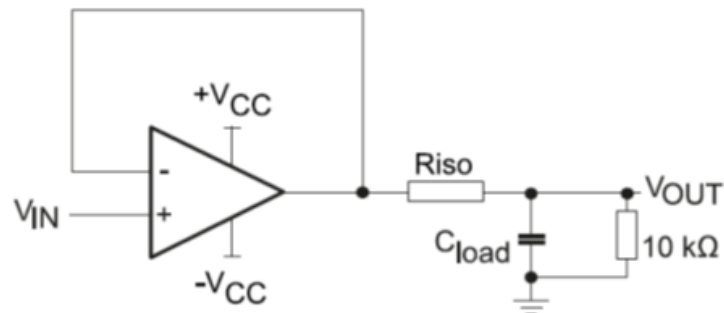
Do not exceed the 150 °C maximum junction temperature for the device. Exceeding the junction temperature limit can cause degradation in the parametric performance or even destroy the device.

5.7 Capacitive load and stability

Stability analysis must be performed for large capacitive loads over 22 pF. Increasing the load capacitance to high values produces gain peaking in the frequency response, with overshoot and ringing in the step response.

Generally, unity gain configuration is the worst situation for stability and the ability to drive large capacitive loads. For additional capacitive load drive capability in unity-gain configuration, stability can be improved by inserting a small resistor R_{ISO} ($10\ \Omega$ to $22\ \Omega$) in series with the output (see Figure 36). This resistor significantly reduces ringing while maintaining DC performance for purely capacitive loads. However, if there is a resistive load in parallel with the capacitive load, a voltage divider is created introducing a gain error at the output and slightly reducing the output swing. The error introduced is proportional to the ratio R_{ISO} / R_L . R_{ISO} modifies the maximum capacitive load acceptable from a stability point-of-view as described in the figure below:

Figure 46. Test configuration for R_{ISO}



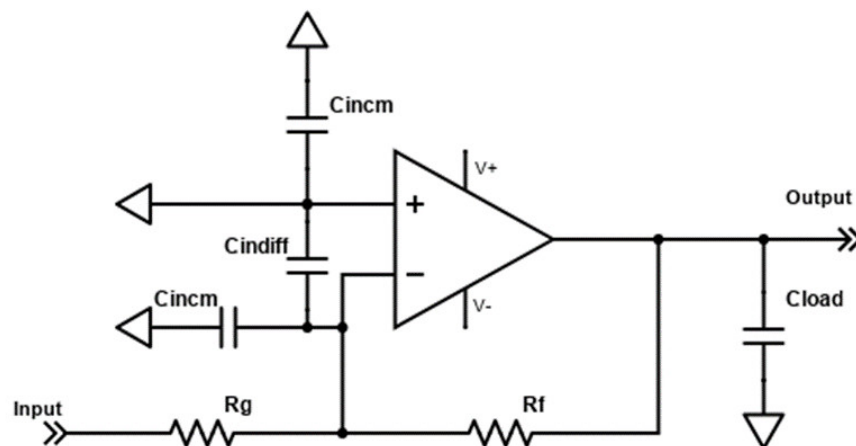
Please note that $R_{ISO} = 22\ \Omega$ is sufficient to make the TSV79x stable whatever the capacitive load.

5.8 Resistor values for high speed op-amp design

Due to its high gain bandwidth product (GBP), this op-amp is particularly sensitive to parasitic impedances. Board parasitics should be taken into account in any sensitive design. Indeed, excessive parasitics (both capacitive and inductive) in the op-amp frequency range can alter performances and stability. These issues can often be mitigated by lowering the resistive impedances.

More specifically, the RC network created by the schematic resistors (R_f and R_g) and the parasitic capacitances of both the op-amp (as documented in Table 5 to Table 7 and illustrated in Figure 46) and the PCB can generate a pole below or in the same order of magnitude than the closed-loop bandwidth of the circuit. In this case, the feedback circuit is not able to fully play its role at high frequency, and the application can be unstable. This issue can happen when the schematic gain is low (typically < 5), or the device is used in follower mode with a resistor in the feedback. In these cases, it is advised to use a low value feedback resistor (R_f), typically $600\ \Omega$.

Figure 47. Inverting amplifier configuration with parasitic input capacitances



Also, some designs use an input resistor on the positive input, generally of the same value than the input on the negative resistor. This resistor can be useful to balance the input currents on the positive and negative inputs, and reduce the impact of those input currents on precision. However, this is not useful on TSV79x as the input currents are very low. Furthermore, this resistor can also interact with the input capacitances to generate a pole. The frequency of this pole should be kept higher than the closed-loop bandwidth frequency.

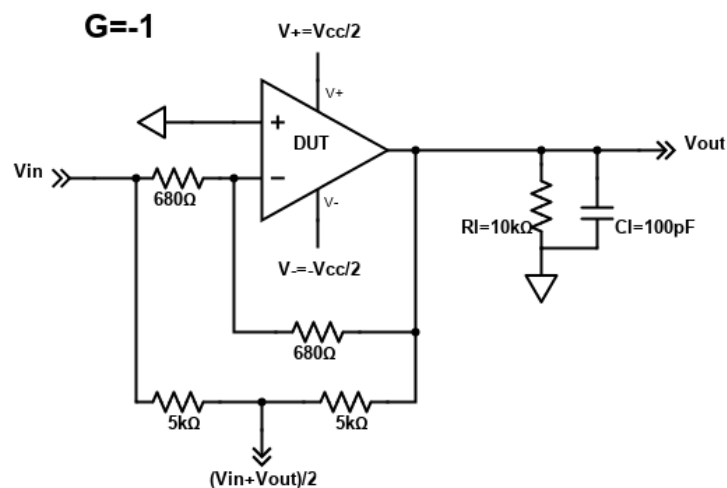
The macromodel provided takes into account the circuit parasitic capacitors. Thus, a transient SPICE simulation (100 mV step) is an easy way to evaluate the stability of the application. However, this cannot replace hardware evaluation of the application circuit.

5.9 Settling time

Settling time in an application can be defined as the amount of time between the input changes, and the output reaching its final value. It is usually defined with a given tolerance, so the output stability is reached when the output stays within the given range around the final value.

In Figure 32 to Figure 35, the settling time is measured in an inverting configuration, using the so-called “false summing node” circuit.

Figure 48. Settling time measurement configuration



This circuit is used with a step input voltage from a positive or negative value, to 0 V. The measurement point being $(V_{in} - V_{out}) / 2$, and V_{out} being in an ideal circuit equal to $-V_{in}$, the measurement point gives half of the error on V_{out} , comparatively to V_{in} . This error is compared to the tolerance, 0.1% for this circuit, to deduce the settling time.

This characteristic is particularly useful when driving an ADC. It is related to the slew rate, GBP and stability of the circuit. It also varies with the circuit gain, the circuit load, and the input voltage step value. However, computing the value of the settling time in a given configuration is not straightforward. The macromodel can give a good estimation, but prototyping can be needed for fine circuit optimization.

5.10 PCB layout recommendations

Particular attention must be paid to the layout of the PCB tracks connected to the amplifier, load, and power supply. The power and ground traces are critical as they must provide adequate energy and grounding for all circuits. The best practice is to use short and wide PCB traces to minimize voltage drops and parasitic inductance. In addition, to minimize parasitic impedance over the entire surface, a multi-via technique that connects the bottom and top layer ground planes together in many locations is often used. The copper traces that connect the output pins to the load and supply pins should be as wide as possible to minimize trace resistance.

5.11 Decoupling capacitor

In order to ensure op-amp full functionality, it is mandatory to place a decoupling capacitor of at least 22 nF as close as possible to the op-amp supply pins. A good decoupling helps to reduce electromagnetic interference impact.

5.12 Macro model

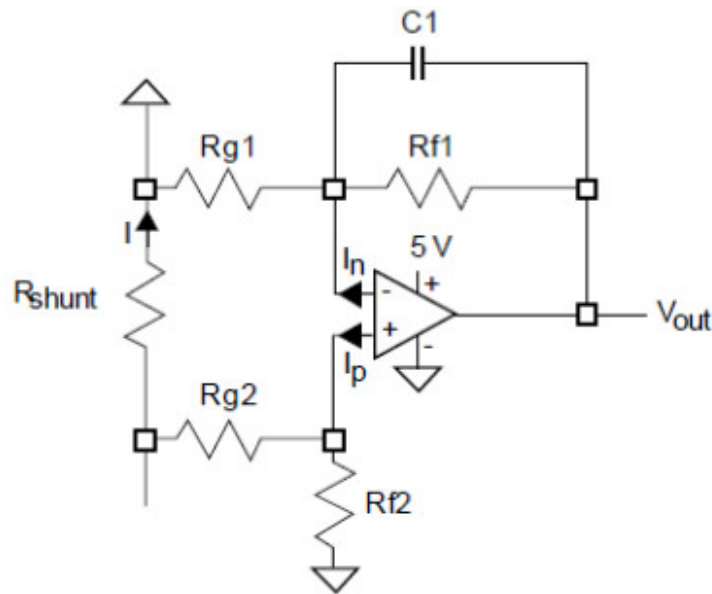
Accurate macro models of the TSV79x device are available on the STMicroelectronics' website at: www.st.com. These models are a trade-off between accuracy and complexity (that is, time simulation) of the TSV79x operational amplifier. They emulate the nominal performance of a typical device at 25 °C within the specified operating conditions mentioned in the datasheet. They also help to validate a design approach and to select the right operational amplifier, but they do not replace onboard measurements.

6 Typical applications

6.1 Low-side current sensing

Power management mechanisms are found in most electronic systems. Current sensing is useful for protecting applications. The low-side current sensing method consists of placing a sense resistor between the load and the circuit ground. The resulting voltage drop is amplified using the TSV79x (see Figure 48).

Figure 49. Low-side current sensing schematic



V_{out} can be expressed as follows:

$$V_{Out} = R_{shunt} \cdot I \left(1 - \frac{R_{g2}}{R_{g2} + R_{f2}} \right) \cdot \left(1 + \frac{R_{f1}}{R_{g1}} \right) + I_p \cdot \frac{R_{g2} \cdot R_{f2}}{R_{g2} + R_{f2}} \cdot \left(1 + \frac{R_{f1}}{R_{g1}} \right) - I_n \cdot R_{f1} - V_{io} \cdot \left(1 + \frac{R_{f1}}{R_{g1}} \right) \quad (10)$$

Assuming that $R_{f2} = R_{f1} = R_f$ and $R_{g2} = R_{g1} = R_g$, Equation 10 can be simplified as follows:

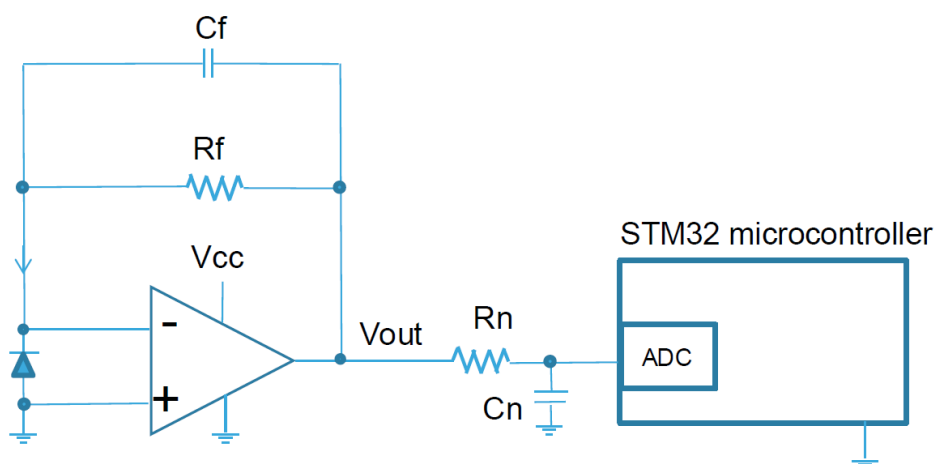
$$V_{Out} = R_{shunt} \cdot I \cdot \frac{R_f}{R_g} - V_{io} \cdot \left(1 + \frac{R_f}{R_g} \right) + R_f \cdot I_{io} \quad (11)$$

The main advantage of using the TSV79x for a low-side current sensing relies on its low V_{io} , compared to general purpose operational amplifiers. For the same current and targeted accuracy, the shunt resistor can be chosen with a lower value, resulting in lower power dissipation, lower drop in the ground path, and lower cost. Particular attention must be paid to the matching and precision of R_{g1} , R_{g2} , R_{f1} , and R_{f2} , to maximize the accuracy of the measurement.

6.2 Photodiode transimpedance amplification

The TSV79x, with high bandwidth and slew rate, is well suited for photodiode signal conditioning in a transimpedance amplifier circuit. This application is useful in high performance UV sensors, smoke detectors or particle sensors.

Figure 50. Photodiode transimpedance amplifier circuit



The transimpedance amplifier circuit converts the small photodiode output current in the nA range, into a voltage signal readable by an ADC following Equation 12:

$$V_{Out} = R_f \cdot I_{photodiode} \quad (12)$$

The feedback resistance is usually in the MΩ range, in order to get a large enough voltage output range. However, together with the diode parasitic capacitance, the op-amp input capacitances and the PCB stray capacitance, this feedback network creates a pole that makes the circuit oscillate. Using a small (few pF) capacitor in parallel with the feedback resistor is mandatory to stabilize the circuit. The value of this capacitor can be tuned to optimize the application settling time with a spice simulation using the op-amp macromodel, or by prototyping.

For more details on tuning this circuit, please read the application note AN4451.

7 Package information

In order to meet environmental requirements, ST offers these devices in different grades of **ECOPACK** packages, depending on their level of environmental compliance. ECOPACK specifications, grade definitions and product status are available at: www.st.com. ECOPACK is an ST trademark.

7.1 SOT23-5 package information

Figure 51. SOT23-5 package outline

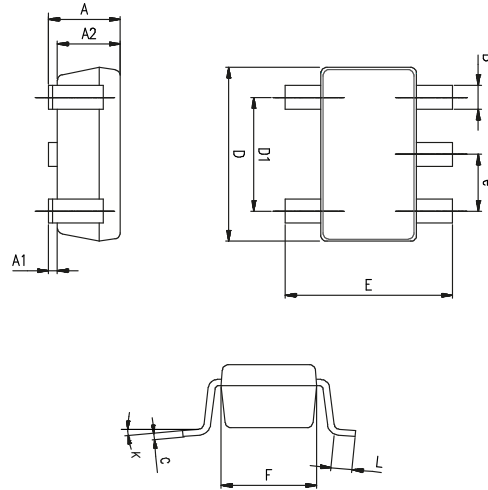


Table 8. SOT23-5 package mechanical data

| Ref. | Dimensions | | | | | |
|------|-------------|------|------|--------|-------|-------|
| | Millimeters | | | Inches | | |
| | Min. | Typ. | Max. | Min. | Typ. | Max. |
| A | 0.90 | 1.20 | 1.45 | 0.035 | 0.047 | 0.057 |
| A1 | | | 0.15 | | | 0.006 |
| A2 | 0.90 | 1.05 | 1.30 | 0.035 | 0.041 | 0.051 |
| B | 0.35 | 0.40 | 0.50 | 0.014 | 0.016 | 0.020 |
| C | 0.09 | 0.15 | 0.20 | 0.004 | 0.006 | 0.020 |
| D | 2.80 | 2.90 | 3.00 | 0.110 | 0.114 | 0.118 |
| D1 | | 1.90 | | | 0.075 | |
| e | | 0.95 | | | 0.037 | |
| E | 2.60 | 2.80 | 3.00 | 0.102 | 0.110 | 0.118 |
| F | 1.50 | 1.60 | 1.75 | 0.059 | 0.063 | 0.069 |
| L | 0.10 | 0.35 | 0.60 | 0.004 | 0.014 | 0.024 |
| K | 0° | | 10° | 0° | | 10° |

7.2 DFN8 2x2 package information

Figure 52. DFN8 2x2 package outline

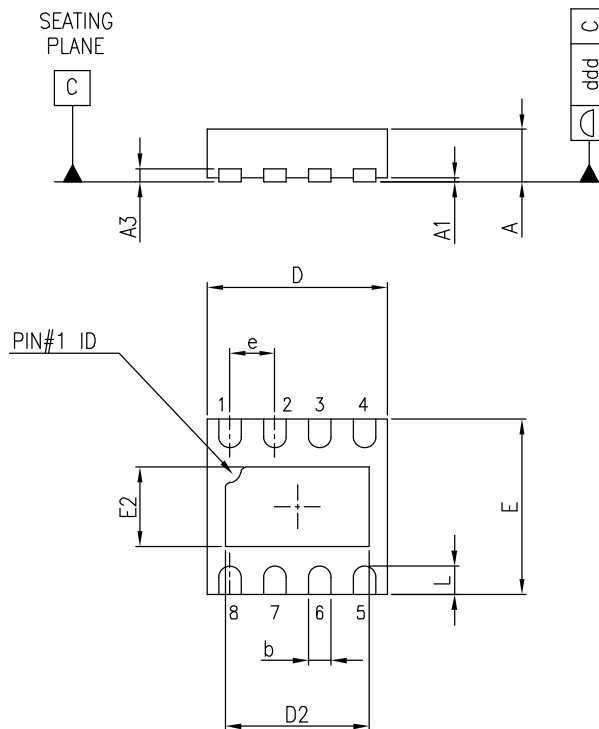
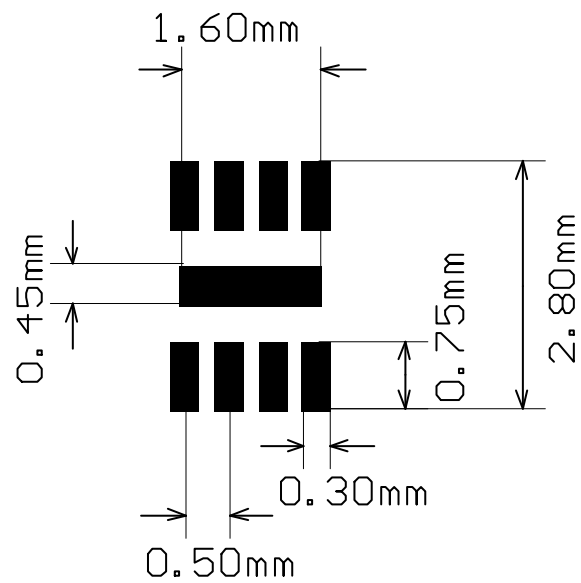


Table 9. DFN8 2x2 package mechanical data

| Ref. | Dimensions | | | | | |
|------|-------------|-------|-------|--------|-------|-------|
| | Millimeters | | | Inches | | |
| | Min. | Typ. | Max. | Min. | Typ. | Max. |
| A | 0.51 | 0.55 | 0.60 | 0.020 | 0.022 | 0.024 |
| A1 | | | 0.05 | | | 0.002 |
| A3 | | 0.15 | | | 0.006 | |
| b | 0.18 | 0.25 | 0.30 | 0.007 | 0.010 | 0.012 |
| D | 1.85 | 2.00 | 2.15 | 0.073 | 0.079 | 0.085 |
| D2 | 1.45 | 1.60 | 1.70 | 0.057 | 0.063 | 0.067 |
| E | 1.85 | 2.00 | 2.15 | 0.073 | 0.079 | 0.085 |
| E2 | 0.75 | 0.90 | 1.00 | 0.030 | 0.035 | 0.039 |
| e | | 0.50 | | | 0.020 | |
| L | 0.225 | 0.325 | 0.425 | 0.009 | 0.013 | 0.017 |
| ddd | | | 0.08 | | | 0.003 |

Figure 53. DFN8 2x2 recommended footprint



Note: The exposed pad of the DFN8 2x2 can be connected to VCC- or left floating.

7.3 MiniSO8 package information

Figure 54. MiniSO8 package outline

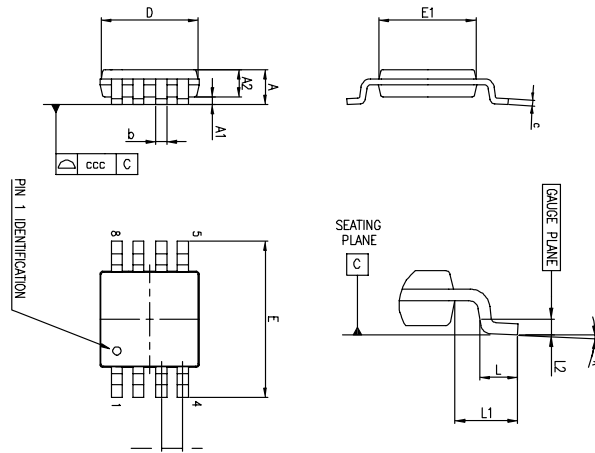


Table 10. MiniSO8 package mechanical data

| Ref. | Dimensions | | | | | |
|------|-------------|------|------|--------|-------|--------|
| | Millimeters | | | Inches | | |
| | Min. | Typ. | Max. | Min. | Typ. | Max. |
| A | | | 1.1 | | | 0.043 |
| A1 | 0 | | 0.15 | 0 | | 0.0006 |
| A2 | 0.75 | 0.85 | 0.95 | 0.030 | 0.033 | 0.037 |
| b | 0.22 | | 0.40 | 0.009 | | 0.016 |
| c | 0.08 | | 0.23 | 0.003 | | 0.009 |
| D | 2.80 | 3.00 | 3.20 | 0.11 | 0.118 | 0.126 |
| E | 4.65 | 4.90 | 5.15 | 0.183 | 0.193 | 0.203 |
| E1 | 2.80 | 3.00 | 3.10 | 0.11 | 0.118 | 0.122 |
| e | | 0.65 | | | 0.026 | |
| L | 0.40 | 0.60 | 0.80 | 0.016 | 0.024 | 0.031 |
| L1 | | 0.95 | | | 0.037 | |
| L2 | | 0.25 | | | 0.010 | |
| k | 0° | | 8° | 0° | | 8° |
| ccc | | | 0.10 | | | 0.004 |

8 Ordering information

Table 12. Order code

| Order code | Channel | Temperature range | Package | Marking |
|------------|---------|---|----------|---------|
| TSV791ILT | 1 | -40 °C to 125 °C | SOT23-5 | K2B |
| TSV792IQ2T | 2 | | DFN8 2x2 | K2B |
| TSV792IST | 2 | | MiniSO8 | K2B |
| TSV792IDT | 2 | | SO8 | TSV792I |
| TSV791IYLT | 1 | -40 °C to 125 °C automotive grade ⁽¹⁾ | SOT23-5 | K227 |
| TSV792IYST | 2 | | MiniSO8 | K227 |
| TSV792IYDT | 2 | | SO8 | TSV792Y |

1. Qualification and characterization according to AEC Q100 and Q003 or equivalent, advanced screening according to AEC Q001 & Q 002 or equivalent are on-going.

Revision history

Table 13. Document revision history

| Date | Revision | Changes |
|-------------|----------|---|
| 11-Nov-2020 | 1 | Initial release. |
| 11-Jan-2021 | 2 | Updated V_{i0} and CMR conditions in Table 7. |
| 26-May-2021 | 3 | Updated V_{i0} and $\Delta V_{i0}/\Delta T$ conditions in Table 6 and Table 7 |

Contents

| | | |
|----------|--|-----------|
| 1 | Pin description | 2 |
| 1.1 | TSV791 single operational amplifier | 2 |
| 1.2 | TSV792 dual operational amplifier | 3 |
| 2 | Absolute maximum ratings and operating conditions | 4 |
| 3 | Electrical characteristics | 5 |
| 4 | Typical performance characteristics | 11 |
| 5 | Application information | 19 |
| 5.1 | Operating voltages | 19 |
| 5.2 | Input offset voltage drift over the temperature | 19 |
| 5.3 | Long term input offset voltage drift | 19 |
| 5.4 | Unused channel | 20 |
| 5.5 | EMI rejection | 20 |
| 5.6 | Maximum power dissipation | 21 |
| 5.7 | Capacitive load and stability | 21 |
| 5.8 | Resistor values for high speed op-amp design | 22 |
| 5.9 | Settling time | 23 |
| 5.10 | PCB layout recommendations | 23 |
| 5.11 | Decoupling capacitor | 24 |
| 5.12 | Macro model | 24 |
| 6 | Typical applications | 25 |
| 6.1 | Low-side current sensing | 25 |
| 6.2 | Photodiode transimpedance amplification | 25 |
| 7 | Package information | 27 |
| 7.1 | DFN8 2x2 mm package information | 28 |
| 7.2 | DFN8 2x2 package information | 29 |
| 7.3 | MiniSO8 package information | 31 |
| 7.4 | SO-8 package information | 32 |
| 8 | Ordering information | 33 |
| | Revision history | 34 |

IMPORTANT NOTICE – PLEASE READ CAREFULLY

STMicroelectronics NV and its subsidiaries (“ST”) reserve the right to make changes, corrections, enhancements, modifications, and improvements to ST products and/or to this document at any time without notice. Purchasers should obtain the latest relevant information on ST products before placing orders. ST products are sold pursuant to ST’s terms and conditions of sale in place at the time of order acknowledgement.

Purchasers are solely responsible for the choice, selection, and use of ST products and ST assumes no liability for application assistance or the design of Purchasers’ products.

No license, express or implied, to any intellectual property right is granted by ST herein.

Resale of ST products with provisions different from the information set forth herein shall void any warranty granted by ST for such product.

ST and the ST logo are trademarks of ST. For additional information about ST trademarks, please refer to www.st.com/trademarks. All other product or service names are the property of their respective owners.

Information in this document supersedes and replaces information previously supplied in any prior versions of this document.

© 2021 STMicroelectronics – All rights reserved

Mouser Electronics

Authorized Distributor

Click to View Pricing, Inventory, Delivery & Lifecycle Information:

[STMicroelectronics:](#)

[TSV791ILT](#) [TSV791IYLT](#)